

Corrosion Protection Properties of Cobalt Salt for Water-Based Epoxy Coatings on 2024-T3 Aluminum Alloy

Thu Thuy Thai^{1,†}, Anh Truc Trinh^{1,3,†}, Gia Vu Pham¹, Thi Thanh Tam Pham², Hoan Nguyen Xuan²

¹*Institute for Tropical Technology, Vietnam Academy of Science and Technology, 18 Hoang Quoc Viet, Hanoi 122000, Vietnam*

²*Faculty of Chemistry, VNU University of Science, Vietnam National University, 19 Le Thanh Tong, Hoan Kiem, Hanoi 110000, Vietnam*

³*Graduate University of Science and Technology, Vietnam Academy of Science and Technology, 18 Hoang Quoc Viet, Hanoi 122000, Vietnam*

(Received November 26, 2019; Revised December 17, 2019; Accepted December 18, 2019)

In this paper, the efficiency and the inhibition mechanisms of cobalt salts (cobalt nitrate and cobalt-exchange silica Co/Si) for the corrosion protection of AA2024 were investigated in a neutral aqueous solution by using the electrochemical impedance spectroscopy (EIS) and polarization curves. The experimental measurements suggest that cobalt cation plays a role as a cathodic inhibitor. The efficiency of cobalt cation was important at the concentration range from 0.001 to 0.01 M. The formation of precipitates of oxides/hydroxides of cobalt on the surface at low inhibitor concentration was confirmed by the Scanning Electron Microscopy/Energy Dispersive X-Ray Spectroscopy (SEM/EDS) analysis. EIS measurements were also conducted for the AA2024 surface covered by water-based epoxy coating comprising Co/Si salt. The results obtained from exposure in the electrolyte demonstrated the improvement of the barrier and inhibition properties of the coating exposed in the electrolyte solution for a lengthy time. The SEM/EDS analysis in artificial scribes of the coating after salt spray testing revealed the release of cobalt cations in the coating defect to induce the barrier layer on the exposed AA2024 substrate.

Keywords: Aluminum alloy, Cobalt-exchange silica, Corrosion inhibition, EIS

1. Introduction

Hexavalent chromium compounds (Cr(VI)) have been effectively applied for corrosion protection of aluminum alloy in various processes such as conversion coating, sealing or rinsing for anodization and in the primer layer... [1-3]. Nevertheless, their cancerous risk and their toxicity for environment required to restrict or eliminate their future use. Significant efforts have been proceeded in last decade to find environmentally friendly alternative inhibitors [4]. Among them, the organic compounds, including the heterocyclic compounds, organic phosphates or carboxylates... and sometimes the synergistic combinations of organic inhibitors have exhibited the high corrosion inhibition effect for the aluminum alloy 2024-T3 surface [5-8]. This effectiveness is based on the formation of a protective barrier film on the surface to avoid the

diffusion of oxygen and aggressive species at the metallic surface. The formed film is on the basis of the electrostatic and chemical adsorption of organic molecules on the metallic surface. However, suffer from the fact that this film is normal unstable caused by the highly reversible adsorption of organic inhibitor, limiting the long-term protection for the metal [9].

The inhibition behavior of inorganic substances such as metal cations toward to the corrosion of aluminum alloys has been variously studied. The lanthanides cations (La, Ce, Y, Pr, Nd, Pm...) have been interested from the 1990s. It was shown that the presence of lanthanum or cerium on the aluminum surface hinder the anodic and cathodic processes [10,11]. The cerium cations gave a highest inhibition effect in comparison with other elements, this is due to the formation of the insoluble cerium hydroxide or cerium oxide film resulted by the reaction with the OH⁻ group during the cathodic process. However, in the chloride medium, composing with the mixture of Ce(OH)₃, Al(OH)₃ and Ce(OH)_xCl_{3-x} is relative thin for corrosion

[†]Corresponding author: anhtruc.trinh@itt.vast.vn (Anh Truc Trinh)

[†]Corresponding author: ttthuy@itt.vast.vn (Thu Thuy Thai)

protection at long time [12-14].

Some transition metal cations like as Mn, Cd, Ni, Co... have been investigated for corrosion protection of aluminum alloys [15-17]. Among them, cobalt has shown an effective potential for inhibiting the corrosion process of metals such as galvanized steel or aluminum alloy [18-22]. Like as chrome, cobalt has multi-valency states and could be easily oxidized. Their corrosion inhibition effect for aluminum and galvanized steel has been investigated. In the alkaline media, it activates as cathodic inhibitor by the formation of Co(OH)_2 precipitation on the metal surface. Co + Ni combination has been used in the bath for sealing during anodization process [23]. Some cobalt salts such as cobalt aluminate (CoAl_2O_4) or cobalt ferrite CoFe_2O_4 were incorporated in the coating for corrosion protection of aluminum alloy and carbon steel respectively [22,24,25]. It was shown that, Co^{2+} could be liberated from the coating matrix to reach the coating/metal interface to form a protective deposition. However, these cobalt salts have not served as expect due to its low solubility in the aqueous solution [24].

In the present work, the efficiency and the inhibition mechanisms of cobalt cations (cobalt nitrate and cobalt-exchange silica Co/Si) for the corrosion protection of AA2024 were investigated in a neutral aqueous solution by using electrochemical impedance spectroscopy (EIS) and polarisation curves. The aim was to better understand the influence of cobalt salts on the corrosion protection and as a consequence, on the leaching process when the salts were incorporated into a coating, which is an important process for the corrosion protection.

In this study, cobalt-exchange silica salt was laboratory synthesized and applied as protective pigment in the water-based epoxy resin for corrosion protection of aluminum alloy 2024.

2. Experiments

2.1 Materials

2024 aluminum alloy (AA2024) is supplied by Sonaca company, Belgium. For the corrosion inhibition measurements in the solution, a rod with naked 1 cm^2 area surface is carefully polished by SiC paper from 80 to 1200 grade, rinsed by absolute ethanol, quickly dried and immediately immersed in the studied solution. The coatings were applied on the AA2024 panel with $4 \times 6 \times 0.1 \text{ cm}$ dimension, before painting the AA2024 samples were cleaned by absolute ethanol and completely dried.

The binder is water-based epoxy resin, comprising YD828 as resin and Epicure 8537 as curing agents. The epoxy coating was deposited on the AA2024 sur-

face by Filmfuge Paint Spinner Ref 110N (Sheen, United Kingdom) equipment.

Cobalt-exchange silica (Co/Si) was laboratory synthesized by protocol following:

Sodium silicate (Sigma Aldrich, 99%) was diluted in mixture $\text{H}_2\text{O}/\text{C}_2\text{H}_5\text{OH}$, then mixed drop-by-drop into 2 M H_2SO_4 solution. After mixing, solution was stirred for 24 h at room temperature then aged at $80 \text{ }^\circ\text{C}$ for 6 h into a reflux system. This step allowed to produce silica gel. Precipitates (Si) were washed with distilled water by centrifugation at the speed of 8000 rpm/min till eliminated totally excessive acid, then dried at $70 \text{ }^\circ\text{C}$ for 24 h.

For cobalt doping, silica particle (Si) was firstly stirred at room temperature in 1 M $\text{Co(NO}_3)_2$ solution (prepared from $\text{Co(NO}_3)_2 \cdot 6\text{H}_2\text{O}$ (Merck, 99%)) for 24 h, then moved to an auto-cooling system at $80 \text{ }^\circ\text{C}$ for 6 h, followed by centrifugation and drying at $70 \text{ }^\circ\text{C}$ for 24 h to obtain cobalt-exchange silica particles (Co/Si).

The Co/Si synthesized was incorporated in the epoxy at 3, 5 and 7 wt% concentration. Co/Si particles were mechanically dispersed in hardener in 1 h before added into epoxy resin. The mixture was continuously stirred for 30 min and sonicated 30 min to assure the completely dispersion of Co/Si before scattering on pre-cleaned aluminum sheets ($40 \times 60 \times 1 \text{ mm}$) with the rotating rate of 500 rpm for 20 s. The film thickness was approximate $30 \pm 4 \text{ } \mu\text{m}$.

2.2 Analytical characterizations

The microstructure of synthesized Co/Si was analyzed by FESEM and XRD (not presented in this paper), the particle size is 100 – 200 nm. The Co content is about 13 wt% (determined by ICP-MS (Inductively Coupled Plasma – Mass Spectroscopy) equipment).

The release of the cobalt cations from Co/Si particles was calculated from the Co concentration of the filtrate during immersion of Co/Si in the electrolyte solution by using UV-vis spectroscopy (GBC Cintra 40).

2.3 Electrochemical measurements

Electrochemical impedance spectroscopy (EIS) measurements were performed using classical three electrodes: the working electrode is the rod of AA2024 or AA2024 panel, an Ag/AgCl/KCl saturated was served as reference and platin grid as counter electrode. The EIS measurements were plotted at the frequency range from 100 kHz to 10mHz at open circuit potential (OCP) with amplitude of 5 mV.

Polarization curves were obtained in the rate of 0.167 mV/s, $\pm 300 \text{ mV}$ from OCP. The electrolyte solution was aqueous solution of 0.05 M NaCl + 0.1 M Na_2SO_4 .

The electrochemical tests were operated with a Biologic SP-300 equipment. The measurements were realized at least three times for each sample for assuring the reproducibility of measurement.

Salt spray test was performed according to ASTM B117 standard. The samples covered by epoxy coating were cross-scratched through the coating using a cutting blade and placed in a salt fog chamber for about 500 h.

3. Results and Discussion

3.1 Corrosion inhibition of cobalt cation for AA2024 surface

The inhibition property of cobalt cation for corrosion of AA2024 surface was firstly characterized by EIS measurements. The EIS results after 2 h of immersion in the solution containing Co^{2+} at different concentration were shown in Fig. 1. A blank sample without cobalt was displayed as reference. In the reference solution, the Bode diagrams of AA2024 have two-time constants, the first around 5 Hz is attributed to the charge transfer occurred on the AA2024 surface during corrosion processes while the second one located in the low frequency domain probably characterizes the diffusion of oxygen [26].

In the presence of cobalt at low concentration (0.001 M), the impedance spectrum has only one time constant in the medium frequency range, characterizing the passive film/electrolyte interface at the A2024 surface. An increase of polarization resistance value was observed when the Co^{2+} concentration increases, at 0.01 M concentration of Co^{2+} , it rises by almost a decade compared to the reference. In fact, after 20 h immersed, electrode surface is strongly attacked while any corrosion products were observed on the surface exposed in the electrolyte solution containing 0.005 M of cobalt nitrate (Fig. 2).

For better understanding the inhibition mechanism of Co^{2+} cation, Fig. 3 shows the polarization curves of AA2024 electrode after 20 h exposure in studied solutions. In comparison with the reference sample, whatever the concentration of Co^{2+} in the solution, a drop of current density in the cathodic branch was clearly identified (Fig. 3a, 3c) while the higher the concentration gave the smaller of the current density in the anodic range (Fig. 3b, 3d). This indicates that the Co^{2+} cation acts as a cathodic inhibitor. This is attributed to the precipitation of $\text{Co}(\text{OH})_2$ in the cathodic site for the formation of an oxide/hydroxide film as mentioned in the literatures [18,19].

The FESEM micrographs of the samples after 20 h exposure are shown in Fig. 4. The reference surface has a thick layer of corrosion products (Fig. 4a). In the presence of 0.01 M of cobalt nitrate, the surface is covered

by a uniform flake-like morphology (Fig. 4b). This petal structure is a typical-hydroxide layer on the AA2024 surface [27]. This hydroxide film formation is activated by Co^{2+} cation, due to the reaction of the Co^{2+} with the hydroxyl generation in the cathodic process. Furthermore, the presence of cobalt in the oxide/ hydroxide layer is clearly shown in the EDS analyses (Fig. 4c). The film formed on the AA2024 surface may act as a diffusion barrier for corrosive species in solution, caused to a decrease of the current density in the anodic range when the cobalt concentration increases from 0.001 to 0.01 M

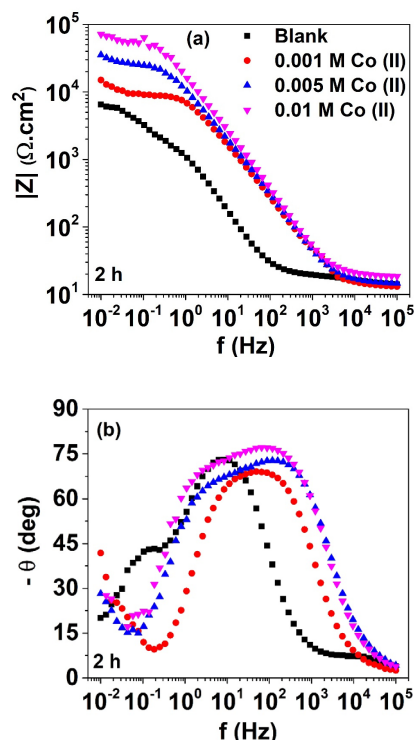


Fig. 1 Impedance diagrams of AA2024 electrode after 2 h exposure in the electrolyte solution and with cobalt nitrate at different concentration.

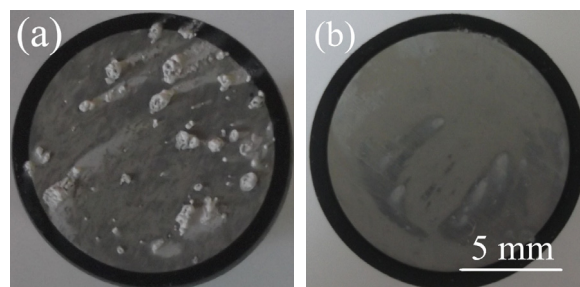


Fig. 2 AA2024 electrode appearance after 20 h of immersion in the electrolyte solution (a) and in the electrolyte solution with 0.005 M $\text{Co}(\text{NO}_3)_2$ (b).

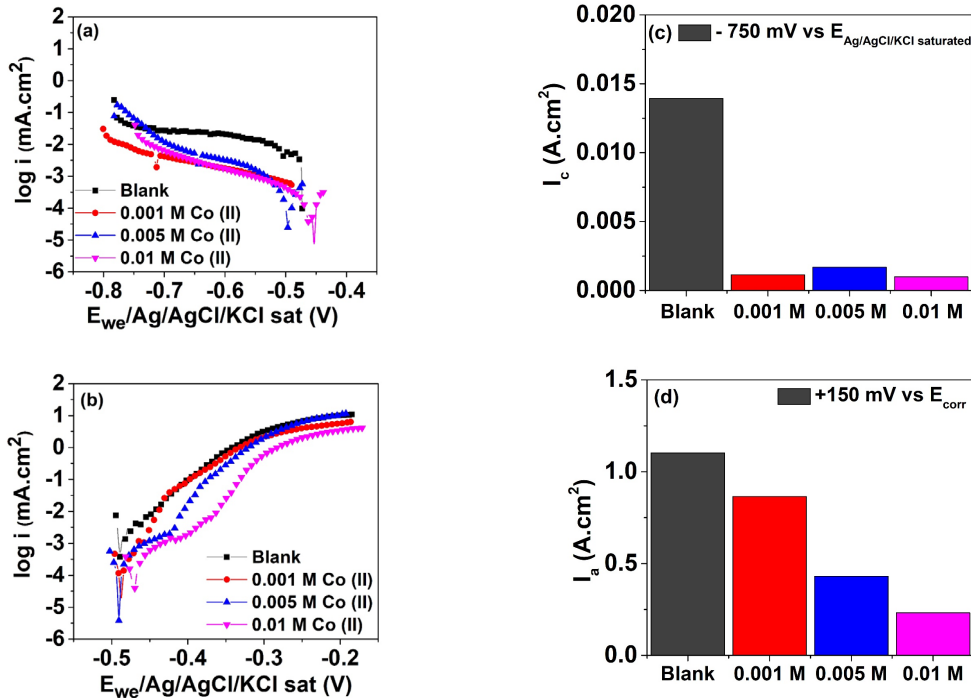


Fig. 3 Polarization curves of AA2024 electrode after 20 h exposure in the electrolyte solution without and with cobalt nitrate at different concentration.

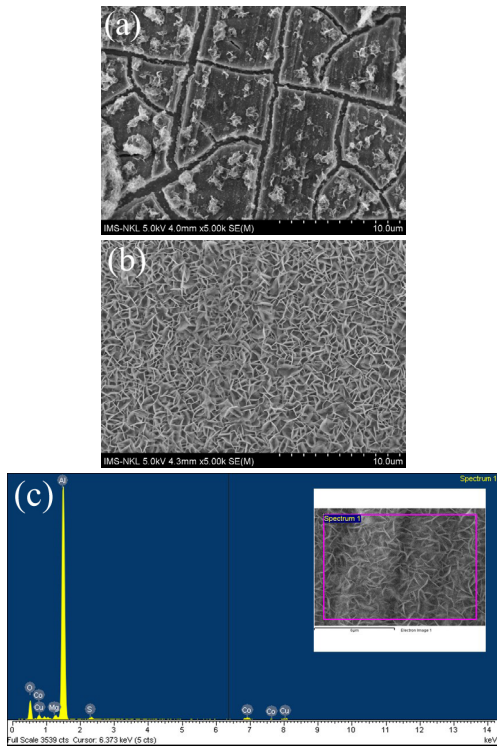


Fig. 4 SEM micrographs on the AA2024 surface after 20 h of exposure in the electrolyte solution (a) and in the electrolyte solution with 0.01 M $\text{Co}(\text{NO}_3)_2$ (b) and EDS data of the sample immersed in the solution containing Co^{2+} (c).

(Fig. 3). In accordance with this observation, previous studies [28,29] have demonstrated the possibility of the formation of a permeation barrier over the surface by the chemical reaction or adsorption of Co^{2+} ions during the oxygen reduction reaction, that generated OH^- at cathodic site. This is effective to reduce the rate of oxygen reduction reaction on AA2024 surface.

3.2 Characterization of the corrosion protection of epoxy coating containing cobalt-exchange silica on the AA2024 surface.

The corrosion protection of epoxy coating containing cobalt-exchange silica (Co/Si) at different concentration was characterized by EIS method. Fig. 5 displays Bode diagrams of the sample covered by epoxy coating in the absence of the Co/Si at different immersion time in the 0.1 M NaCl solution. Regarding different curves, the system evolves with the immersion time. Two time-constants are well observed on the phase of the impedance diagram. The first one located in the high frequency range corresponds to the coating and the second at low frequency relates to the corrosion process on the AA2024 surface [30]. The modulus of the impedance associated with both those time-constants is continuously dropped during immersion. This behavior indicates that the coating degrades rapidly in contact with the electrolyte. It is shown

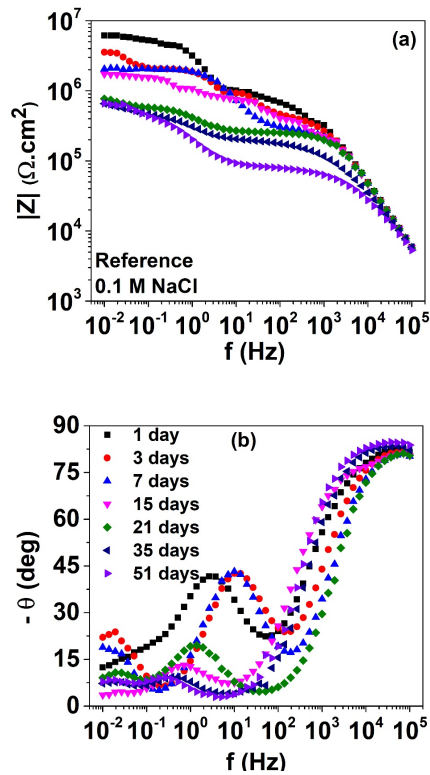


Fig. 5 Bode diagrams obtained for AA2024 surface covered by the epoxy coating (reference sample) during immersion time in the NaCl 0.1 M solution.

in the phase diagram, the second time-constant appeared as soon as 1 day immersed.

Fig. 6 summarizes the Bode diagrams of the samples coated by epoxy coating loading with Co/Si at concentration of 3 wt% (Fig. 6a, b), 5 wt% (Fig. 6c, d) and 7 wt% (Fig. 6e, f) during immersion time. The impedance curves present one time-constant at high frequency, the behavior at low frequency is not well defined for the system loading Co/Si. It seems that the corrosion process has been slowed down at the AA2024 surface beneath the coating containing Co/Si. At low content of the Co/Si (3 wt%), the progressive decrease of the impedance modulus is observed but at higher concentration, the impedance sharp and the impedance modulus are not modified with immersion time, this is more remarkable at concentration of 7 wt%.

For better comparison, the film resistance values (R_f) were graphically calculated and the evolution of the R_f and the modules values at low frequency ($|Z|_{26.8\text{mHz}}$) during immersion times are reported in Fig. 7. The R_f value of the coating without Co/Si at the beginning of immersion is higher in comparison with the coating with Co/Si, this is due to the porosity of the coating in presence of the additive (Fig. 7a). However, for 7 days of immersion, it drastically decreases to reach the R_f value lower than in the system loading Co/Si. The R_f values of the coating

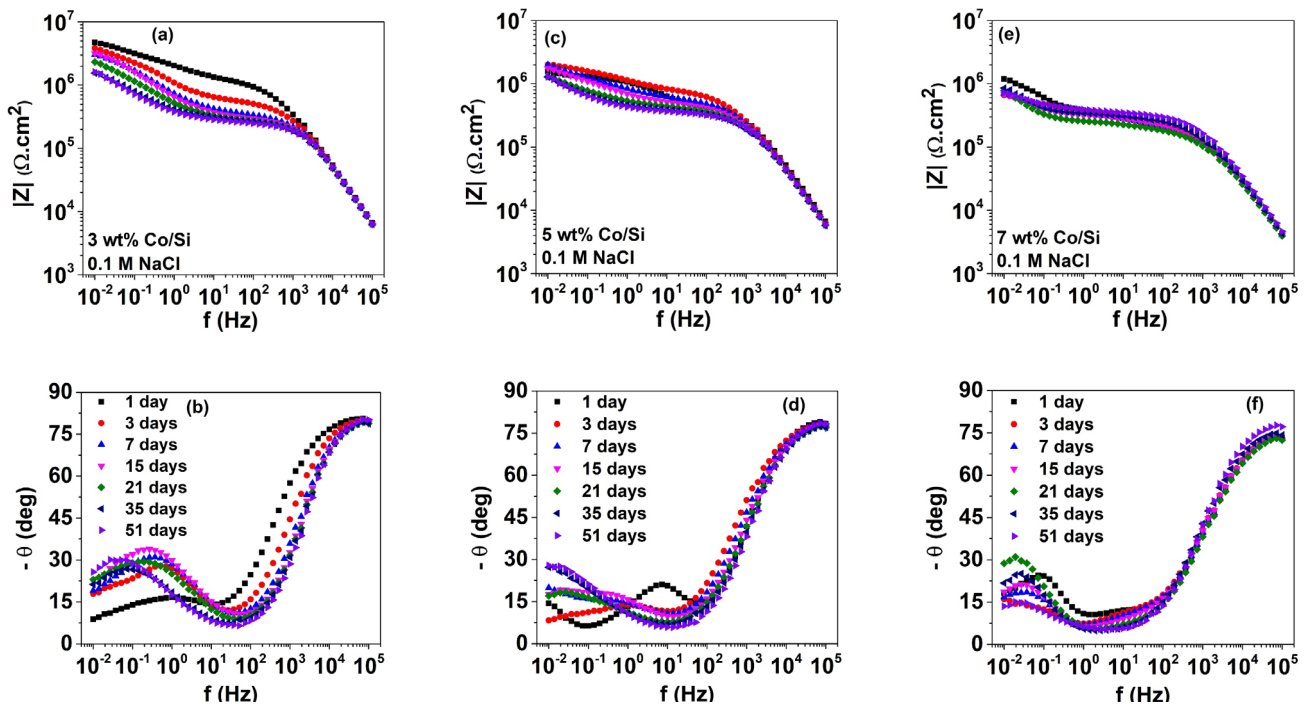


Fig. 6 Bode diagrams obtained for AA2024 surface covered by the coating loaded 3, 5 and 7 wt% Co/Si during immersion time in the NaCl 0.1 M solution.

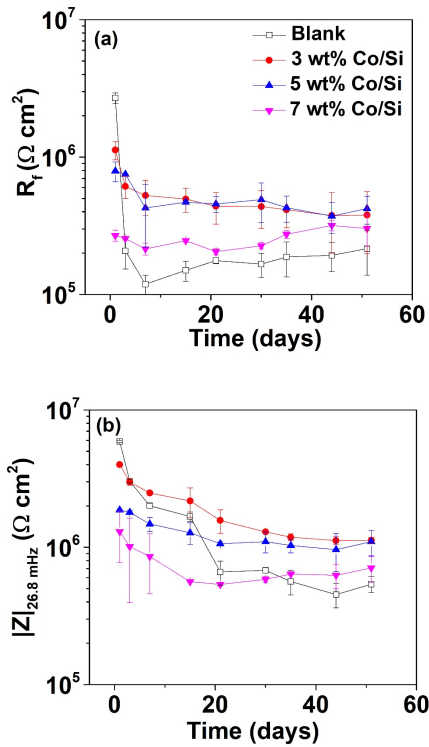


Fig. 7 Evolution of the R_f value (a) and impedance modulus value $|Z|_{26.8 \text{ mHz}}$ (b) during immersion time.

with Co/Si are lower than the neat epoxy coating in the first day but remain relatively stable with immersion time. After 56 days of immersion, the approximate R_f value is around $5.10^{-5} \Omega \cdot \text{cm}^2$, five times higher than the neat epoxy for all studied concentrations. The variation of modulus value at low frequency ($|Z|_{26.8 \text{ mHz}}$) (Fig. 7b) has the same trend with the evolution of the R_f value. The reference sample rapidly degraded while the sample loading gave the low $|Z|_{26.8 \text{ mHz}}$ value at beginning but remained high for long time of immersion. This shows the protection property of the coating in presence of the Co/Si, but it is remarked that the high content of the Co/Si (7 wt%) provides a lower protection in compared with the other concentration (3 and 5 wt%).

In order to understand the activity of Co^{2+} cations in the coating, the release of Co^{2+} cations from Co/Si particles has been measured. Fig. 8 presents the UV-vis spectra of different concentration of cobalt ions in the electrolyte (Fig. 8a) and the release of cobalt cations from Co/Si particles versus immersion time in the electrolyte solution (Fig. 8b). It is clearly seen in Fig. 8b, Co^{2+} cations were massively liberated to the electrolyte solution. This observation reflects the fact that the Co^{2+} cations may be released as soon as the penetration of the electrolyte

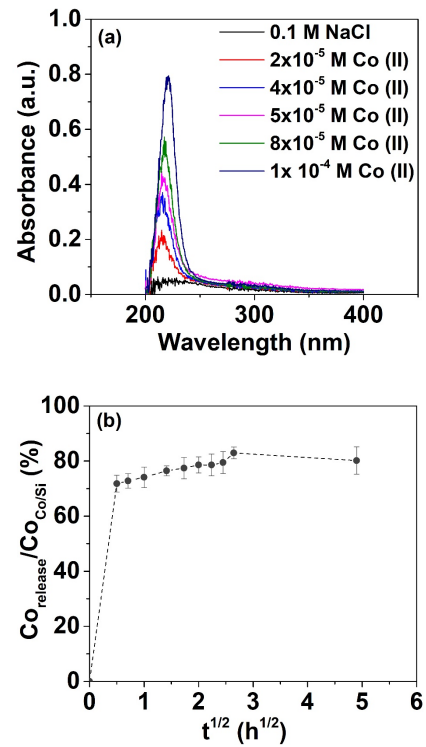


Fig. 8 UV-vis spectra of Co (II) ions determined in 0.1 M NaCl and release of cobalt cations from Si/Co in function of stirring time.

through the epoxy coating to coating/AA2024 interface. By the fast leaching of the Co^{2+} cations, for only 1 day immersed, the film resistance of three samples loaded Co/Si showed the values lower in compared with the reference without Co/Si as observed in Fig. 8. In the other hand, the Co^{2+} cations leaching at corrosion sites could lead to cathodic inhibition which would limit the local responsiveness. In addition, associating with the formation of the hydroxide/oxide products, the film resistance is maintained for long immersion (56 days). This phenomenon is clearly observed for the high loading content of Co/Si (7 wt%), the film resistance increases with immersion time. This increase of R_f is attributed to the massive liberation of the Co^{2+} cations, reacting to form the oxide/hydroxide deposition on the interface and sealing the suitable bottom pores of the coating.

Salt spray method was performed as accelerated test for the AA2024 panel coated by epoxy coating pigmented with Co/Si salt at 5 wt% concentration. SEM micrographs of the specimen for 500 h of exposure were presented in Fig. 9, a blank sample without Co/Si was shown as reference. No blister was observed around scratches for both sample with and without Co/Si, demonstrating a good adherence of epoxy coating. The corrosion products were

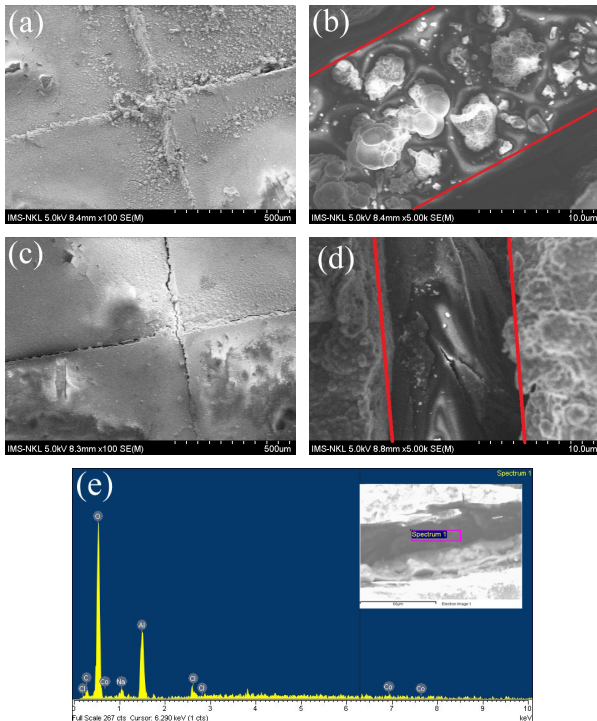


Fig. 9 SEM micrographs of scribed coated AA2024 samples after 500 h of salt spray test (a, b) coating without Co/Si (c, d) coating loading 5 wt% of Co/Si (e) EDS analyze on the bottom of the scribe for the sample with 5 wt% Co/Si.

entirely filled inside the scratches for the reference (Fig. 9a) while a few products appeared underneath the scratches for the sample with Co/Si (Fig. 9c). This observation is evident in the higher magnification, an accumulation of the corrosion products can be seen in the blank sample (Fig. 9b). A thin film associated with the traces of cobalt detected in Fig. 9e indicates that the corrosion process is limited in the bottom of the scribed area for the sample containing Co/Si. This is due to the inhibition effect of the cobalt cations, which were leached from the coating during the test.

The EIS measurements and salt spray tests reveal that in the coating, the presence of Co/Si salt could reinforce the coating/AA2024 interface and maintain the corrosion protection of the coating. However, it would be better to control the release of cobalt cations for the leaching and inhibiting on demand of the cations in the coating.

4. Conclusions

In the electrolyte solution, Co^{2+} cations limit the corrosion process of aluminum alloy 2024 mainly in the local alkaline cathodic site for reinforcing the hydroxide/oxide layer on the AA2024 surface even in low concentration

(0.001 M). This action of Co ions based on the reduction of mass-transfer-limited current densities linked with oxygen reduction at cathodic reaction. On the other hand, due to the adsorption ability with oxide metal, Co^{2+} ions can reinforce passive barrier layer with Al, O_2 formed at surface metallic. By the improvement of surface deposit layer, the anodic current decreases at high concentration of cobalt.

The Co^{2+} cations could rapidly leach from the cobalt-exchange silica (Co/Si) to electrolyte solution. By the way, in the coating, it releases as soon as the penetration of the electrolyte solution to reach the coating/metal interface. The reaction of the Co^{2+} cations in the interface could improve the hydroxide/oxide layer on the AA2024 surface and then clog the bottom pores in the coating to maintain the barrier effect during the test.

Acknowledgements

The authors thank VAST for the funding support under project NVCC13.06/19-19.

References

1. I. M. Zin, R. L. Howard, S. J. Badger, J. D. Scantlebury, and S. B. Lyon, *Prog. Org. Coat.*, **33**, 203 (1998).
2. M. Kendig, S. Jeanjaquet, R. Addison, and J. Waldrop, *Surf. Coat. Technol.*, **140**, 58 (2001).
3. J. Vander Kloet, W. Schmidt, A. W. Hassel, and M. Stratmann, *Electrochim. Acta*, **48**, 1211 (2003).
4. R. L. Twite and G. P. Bierwagen, *Prog. Org. Coat.*, **33**, 91 (1998).
5. G. Williams, A. J. Coleman, and H. Neil Mc Murray, *Electrochim. Acta*, **55**, 5947 (2010).
6. G. Boisier, N. Portail, and N. Pèbère, *Electrochim. Acta*, **55**, 6182 (2010).
7. S. J. Garcia, T. A. Markley, J. M. C. Mol, and A. E. Hughes, *Corros. Sci.*, **69**, 346 (2013).
8. S. Marcelin and N. Pèbère, *SCorros. Sci.*, **101**, 66 (2015).
9. P. Visser, H. Terry, and J. M. C. Mol, *Corros. Sci.*, **140**, 272 (2018).
10. H. Allachi, F. Chaouket, and K. Draoui, *J. Alloy. Compd.*, **475**, 300 (2009).
11. M. Bethencourt, F. J. Botana, J. J. Calvino, M. Marcos, and M. A. Rodríguez-Chacón, *Corros. Sci.*, **40**, 1803 (1998).
12. A. J. Aldykiewicz Jr., H. S. Isaacs, and A. J. Davenport, *J. Electrochem. Soc.*, **142**, 3342 (1995).
13. A. Davenport, H. Isaacs, and M. Kendig, *J. Electrochem. Soc.*, **136**, 1837 (1989).
14. M. Dabala, L. Armelao, A. Buchberger, and I. Calliari,

- Appl. Surf. Sci.*, **172**, 312 (2001).
15. M. G. A. Khedr and A. M. S. Lashien, *Corros. Sci.*, **33**, 137 (1992).
 16. M. Mahdavian and M. M. Attar, *Corros. Sci.*, **51**, 409 (2009).
 17. A. C. Balaskas, M. Curioni, and G. E. Thompson, *J. Electrochem. Soc.*, **161**, C389 (2014).
 18. H. Leidheiser Jr. and I. Suzuki, *J. Electrochem. Soc.*, **128**, 242 (1981).
 19. H. Leidheiser Jr. and G. W. Simmons, *J. Electrochem. Soc.*, **129**, 1658 (1982).
 20. A. G. Muñoz, *Corros. Sci.*, **47**, 2307 (2005).
 21. J. Xiong, D. K. Sarkar, and X-G. Chen, *Appl. Surf. Sci.*, **407**, 361 (2017).
 22. N. Soltani, H. Salavati, and A. Moghadasi, *Surf. Interface.*, **15**, 89 (2019).
 23. F. Snogan, C. Blanc, G. Mankowski, and N. Pebere, *Surf. Coat. Technol.*, **154**, 94 (2002).
 24. E. Ghasemi, B. Ramezanzadeh, S. Saket, and S. Ashhari, *J. Coat. Technol. Res.*, **13**, 97 (2016).
 25. M. Amiri1, M. Salavati-Niasari1, A. Akbari1, and R. Razavi, *J. Mater. Sci.: Mater. Electron.*, **28**, 10495 (2017).
 26. P. Rodič, I. Milošev, M. Lekka, F. Andreatta, and L. Fedrizzi, *Electrochim. Acta*, **308**, 337 (2019).
 27. M. Richetta, *J. Material Sci. Eng.*, **6**, 1000397 (2017).
 28. M. A. Jakab, F. Presual-Moreno, and J. R. Scully, *J. Electrochem. Soc.*, **153**, B244 (2006).
 29. H. Tamura, N. Katayama, and R. Furuichi, *J. Colloid Interf. Sci.*, **195**, 192 (1997).
 30. K. Bonnel, C. Le Pen, and N. Pebere, *Electrochim. Acta*, **44**, 4259 (1999).